Journal of Quantitative Spectroscopy & Radiative Transfer 236 (2019) 106601

Contents lists available at ScienceDirect

Journal of Quantitative Spectroscopy & Radiative Transfer

journal homepage: www.elsevier.com/locate/jqsrt

Light scattering in a spatially-correlated particle field: Role of the radial distribution function

Corey D. Packard [a,b], Michael L. Larsen [a,c], Will H. Cantrell [a], Raymond A. Shaw [a,*]

[a] Department of Physics and Atmospheric Sciences Program, Michigan Technological University, 1400 Townsend Drive, Houghton, MI 49931, USA
[b] ThermoAnalytics, Inc., 23440 Airpark Blvd., Calumet, MI 49913, USA
[c] Department of Physics and Astronomy, College of Charleston, 66 George Street, Charleston, SC 29424, USA

ARTICLE INFO

Article history:
Received 18 March 2019
Revised 2 August 2019
Accepted 2 August 2019
Available online 03 August 2019

Keywords:
Spatial correlation
Particle clustering
Light scattering
Monte Carlo Ray Tracing
Radial distribution function
Radiative transfer

ABSTRACT

Radiative transfer through particle-laden media such as clouds can be impacted by variations in particle spatial distributions. Due to mixing and inertial effects of droplets suspended in the almost always turbulent atmosphere, cloud particles are often spatially-correlated. The correlations result in clusters and voids within the droplet field that, even when smaller than the photon mean free path, can lead to deviations from the exponential extinction law. Prior work has numerically investigated these departures from exponential attenuation in absorptive media; this work extends those results for a scattering medium. The problem is explored with a Monte Carlo Ray Tracing (MCRT) program capable of tracking light attenuation through both perfectly random (uncorrelated) and spatially correlated collections of scatterers and/or absorbers. The MCRT program is favorably compared to two-stream flux equations, and numerical exploration of the pure-absorption case is used to determine the sampling statistics necessary to characterize radiative transmission within the numerical simulation. Light transmission through fields of spatially-correlated, non-absorbing, scattering particles is explored. Particles are distributed following a Matérn Point Process, which allows cluster strength and size, as well as the usual variables of particle scattering cross section and number density to be varied. The results show that the degree of non-exponential attenuation is determined by the magnitude and shape of the radial distribution function, which describes correlations in discrete (non-continuous) particle distributions. Parametric studies revealed that the number of clusters and cluster radius, factors in the Matérn radial distribution function, impact direct, diffuse and backward radiative transfer. The Matérn RDF is shown to be consistent with a previous "cloudlet" approach, providing a bridge between the analytical cloudlet model and continuous correlation function approaches.

1. Introduction

Radiative transfer through a spatially correlated medium results in a distinct behavior, essentially because photons propagate further in void regions, and experience stronger extinction in dense regions, relative to a homogeneous medium [30]. The problem has a multitude of applications, ranging from the cloudy atmosphere to biological and energy-generation systems [13,22,51]. In this work, we consider distributions of discrete particles, with the atmospheric context as our motivating problem.

When spatial correlations are present in the positions of perfectly absorbing particles, deviations from the usual exponential extinction emerge [15,20,23]; these deviations can be both super- or sub-exponential, depending on the nature of the spatial correlations [44]. Spatial correlations between particles within a turbulent flow can be created by several mechanisms, including inertial clustering [41] and turbulent mixing [48]. For example, mixing and entrainment in atmospheric cloud boundaries leads to pockets of cloudy and clear air on spatial scales ranging from km to mm [14,43]. Recent work has suggested that, at least in the absorbing-particle problem, the relevant clustering metric is the radial distribution function [15,44].

How does the situation change when we consider diffuse radiation in a scattering medium? Previous results were for absorbing particles or, equivalently, extinction of a direct beam, and we might expect that the situation with scattering is more complex. Nevertheless, the key geometrical argument that suggests a mechanism for the non-exponential behavior should be general (see, e.g., [19,20]), and a natural follow-on question to the previous numer-

* Corresponding author.
E-mail address: rashaw@mtu.edu (R.A. Shaw).

https://doi.org/10.1016/j.jqsrt.2019.106601
0022-4073/

ical work on absorbing clouds is to determine whether the radial distribution function can also capture the essential physics at play in a medium containing purely scattering particles.

We address the problem using the ray tracing Monte Carlo radiative transfer approach that has been shown to be consistent with standard radiative transfer (e.g., [3]). This should be consistent with the findings of Mishchenko [35,36] that even in a correlated medium the classical radiative transfer equation holds, as long as high-order scattering paths can be neglected and assumptions of ergodicity and spatial uniformity are valid. To limit the scope of the work, we take as context the transport of visible light in a cloud of water droplets as found in atmospheric applications (e.g., wavelength $\sim$550 nm and droplet radius $\sim$14 µm). In this regime, absorption is extremely weak and therefore in the remainder of this work we take the single scatter albedo to be exactly unity. Furthermore, we consider the regime in which multiple scattering does not become dominant (e.g., optical thickness of order unity).

There are several reasons motivating the use of Monte Carlo Ray Tracing (MCRT) within a field of discrete particles rather than the more standard (and computationally efficient) photon-path-distribution function. At a fundamental level, we are exploring radiative transfer at scales on which the notion of a continuously-distributed system becomes ill-defined, and where discreteness effects such as sampling or 'shot' noise are relevant. We therefore take the direct approach of explicit representation of each particle. Another primary motivation is generality and flexibility when it comes to representing radiative transfer in a real system, such as the Pi Cloud Chamber [6]. In that case, we must consider sampling of a dilute medium within a confined geometry. We find the possibility of future comparison between numerical computations of direct and diffuse radiation and measurements of these fields in a laboratory cloud chamber appealing; in particular, we have in mind the Pi Cloud Chamber, which is able to produce optical thicknesses of order unity [6]. For example, the assumptions drawn into focus by Mishchenko merit direct experimental assessment, especially the insight that averaging scales play a central role [36]. Besides the finite-sample effects, the explicit, discrete-particle approach allows for simpler implementation of boundary conditions. The generality of this approach will also allow the method to be applied to conditions in which clustering may not be isotropic, such as in turbulent Rayleigh-Bénard convection. Eventually, it would be of interest to compare the discrete approach to the path-distribution approach for dilute, finite-size systems.

In this work, perfectly random and correlated spatial particle distributions (generated using a Matérn Point Process model, having a known closed-form radial distribution function) are generated within a simulation volume. Then, a Monte Carlo Ray Tracing code – capable of simulating scattering events either through full Mie computation or more approximately through the Henyey-Greenstein phase function – propagates individual photons through the simulation volume, tracking direct, diffuse forward, and diffuse backward radiative fluxes from an initially collimated beam of photons entering the simulation volume at normal incidence.

The paper proceeds as follows: In Section 2 we define the radial distribution function (RDF) and introduce the Matérn process as an analytic model for introducing particle spatial correlations via the RDF. In Section 3 we describe the Monte Carlo Ray Tracing (MCRT) code that is used to simulate light propagation through a medium containing discrete particles. In Section 4 we present results of the simulations, showing departure from propagation through a uniformly random particle field, and we interpret the results in the context of the RDF. In the concluding section we discuss the results and their possible implications for atmospheric radiative transfer.

2. Exploring the Matérn cluster process

2.1. The influence of particle clustering on transmission through a scattering medium

As noted above, deviations from exponential attenuation in traditional radiative transfer theory are expected when the particles in the medium are spatially correlated [20]. Inertial particles in a turbulent fluid (e.g., cloud droplets in the atmosphere) provide one physical scenario where these spatial correlations are known to exist [26,42]. Previous work [15,23,44] suggests that the deviation from exponential behavior in such media may depend on the radial distribution function describing that statistical structure of particulate clustering.

The radial distribution function $g(r)$ of a particle-laden medium quantifies the scale-localized clustering of the particles in the medium [21,25,26,41,42,44]. It can be readily understood through its relation to the joint probability of finding a particle in volumes dV_1 and dV_2, both separated by distance r, in a system with global particle number density n:

$$p_{(1,2)}(r) = (ndV_1)(ndV_2)\ g(r) \tag{1}$$

Algorithmically, $g(r)$ can be understood as the observed number of particle pairs separated by distance $r \pm \delta r$ relative to the number of particle pairs expected at the same distance for a perfectly random population (Poisson distributed at all scales).

Testing the radial distribution function dependence on radiative transmission through a purely *scattering* medium will be facilitated by generating scatterer positions within the simulation volume via a method that produces a known, closed-form radial distribution function. Particle positions in a turbulent flow-field in steady-state are often modelled with a decaying power-law RDF that is dependent on the Stokes number [8]. The construction of a simulation volume of scatterers with a power-law radial distribution function presents at least two challenges; (i) $g(r \to 0) = \infty$, which is physically impossible, and (ii) the lack of a simple algorithm to place particles in a way that replicates a power-law radial distribution. Additionally, there are some physical mechanisms that cause clustering that are not expected to have a power-law form like particle charging [28] or convective organization [2]. For this study, in lieu of generating clustered particle spatial locations for a specific physical mechanism (e.g., running turbulence simulations), we instead take a more general approach. We have opted to utilize the Matérn cluster process to distribute scattering particles throughout the simulation volume, which has the advantage of providing an analytical form for the RDF that can be explicitly adjusted to change the scale and magnitude of clustering.

The Matérn cluster process [31–33] is a Neyman–Scott point process model that has several advantageous features for this work: (i) it has an analytically straightforward closed-form expression for its radial distribution function, (ii) it has a fundamental characteristic length-scale R, and (iii) it is numerically easy to simulate. For spatial scales larger than $2R$, the Matérn cluster process radial distribution function is the same as that for a perfectly random distribution. Additionally, like power-law RDFs, the RDF of the Matérn cluster process has a monotonic decrease with increasing spatial scale (but does not diverge at small distances like power-law RDFs).

2.2. Construction and properties of a Matérn cluster process

All Neyman–Scott point process models are constructed in the same way; (i) some number of "parent" particles N_p, are distributed in a perfectly random manner throughout the cloud volume V with spatial density N_p/V, (ii) some discrete probability distribution function with a specified mean λ_D is sampled to assign

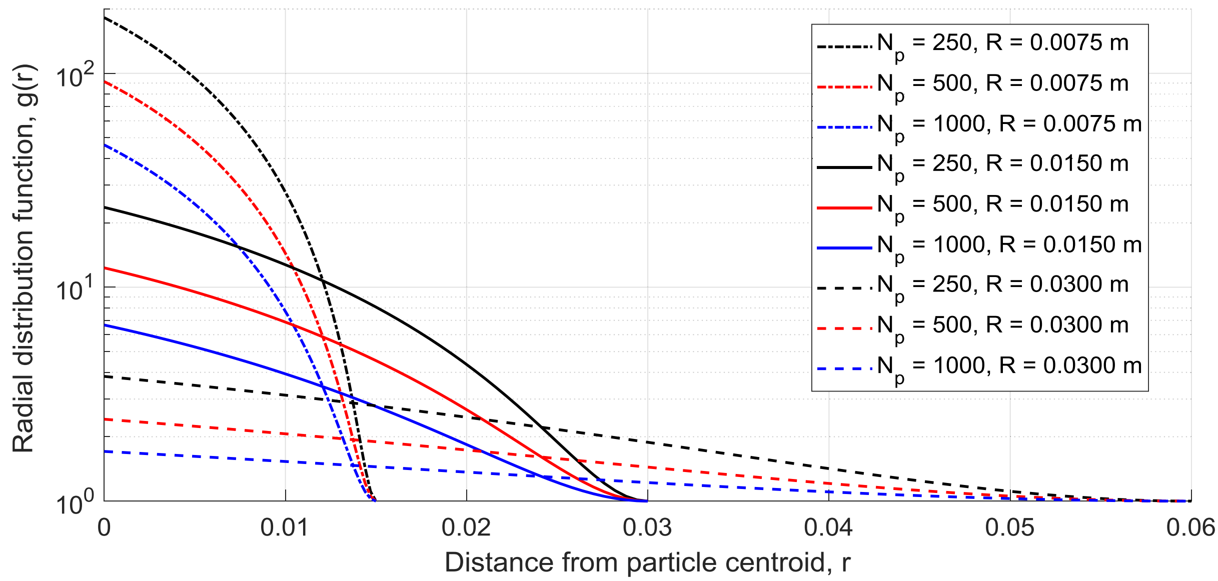

Fig. 1. Dependence of theoretical Matérn radial distribution function (RDF) on number of clusters, N_p, and cluster radius, R, given the 0.08 m^3 cloud volume used in our simulations. Note that at distances r greater than $2R$ the RDF illustrates statistical structure equivalent to an uncorrelated distribution ($g_{3D} = 1$ for $r > 2R$).

how many "daughter" particles will be associated with each parent particle, and (iii) some continuous probability density function is sampled to determine how far each daughter particle is placed from its associated parent particle. The final collection of particles will be the ensemble of daughter particles generated through this process. For the Matérn cluster process, the discrete probability distribution in step (ii) is a Poisson distribution and the continuous probability distribution in step (iii) is designed to place the daughter with uniform probability anywhere within a sphere of radius R around the associated parent particle. Ultimately, a statistically homogeneous but clustered distribution with approximately ($N_p \bullet \lambda_D$) total particles is generated. More detail including a figure demonstrating this construction process in two-dimensions can be found in Larsen et al. [24]. For this system, the resulting radial distribution function $g_{3D}(r)$ for a 3-dimensional Matérn cluster process can be written [7,24]

$$g_{3D}(r) = \begin{cases} \dfrac{3V}{8\pi R^6 N_p}\left(R - \dfrac{r}{2}\right)^2 \left(2R + \dfrac{r}{2}\right) + 1 \;\; (r < 2R) \\ 1 \;\; (r \geq 2R) \end{cases} \tag{2}$$

It is important to note here that with a constant cloud volume, the Matérn radial distribution function (RDF) given by Eq. (2) is dependent only on the number of parent clusters and the cluster radius (N_p and R, respectively), and does not vary with the average number of particles per cluster, λ_D. The dependence of the Matérn RDF, $g(r)$, on N_p and R is illustrated in Fig. 1.

3. Description and validation of Monte Carlo Ray Tracing code

3.1. Overview of the MCRT code ('mcScatter')

A Monte Carlo scattering simulation code, 'mcScatter', was created to explore the role that spatial correlations play in radiative transfer through a light-scattering medium such as an atmospheric cloud. The general structure of our MCRT code was motivated in part by a desire to eventually validate the numerical results with experiments in a cloud chamber facility [6]. The virtual laboratory of a computer simulation allows for the relaxation of the physical constraints of an actual cloud chamber (such as particle clustering limits and experimental setup restrictions) to predict experimental results and develop an effective methodology for measuring parameters of interest.

To match experimental conditions potentially realizable in the chamber, the numerical work that follows is limited to a spatial domain of 2 m x 0.2 m x 0.2 m (inspired by a realistic optical path through the chamber) and total optical thickness of order $\tau^* \sim 1$. Our MCRT code, described in greater detail in the supplemental material, allows for the specification of optical wavelength, particle size, complex index of refraction and many other boundary conditions. In this paper we focus our analysis in the visible spectrum with an optical wavelength of 550 nm, and examine relatively large but realistic cloud droplet sizes (e.g., radius ~14 µm) based on previous cloud chamber measurements [6,38]. The resulting size parameter focuses our analysis on the forward-scattering regime with a single scatter albedo of 1 and a scattering efficiency of $Q_{sca} \approx Q_{ext} \approx 2$.

Approaches exist for addressing this problem directly from Maxwell's equations [35,37]; however, direct use of methods like the superposition T matrix method remain impractical for systems with large numbers of particles like clouds. Previous work [5,12,39] has led to the development of heuristic models to quantify the radiative transmission through inhomogeneous particle-laden media via a variety of methods. In Section 5 we discuss the ability of these heuristic techniques to predict results similar to those found by our MCRT analysis.

Others have investigated such heterogeneous systems through the development of numerical Monte-Carlo simulations [29,30]; a clear discussion can be found in Bohren and Clothiaux [3] but numerous relevant publications can be found on the subject [10,11,40]. The Monte Carlo method [46] has often been applied to investigate radiative transfer problems where closed form solutions are challenging or impossible, and a detailed description of its application to inhomogeneous media has been presented [9].

These numerical methods typically explore radiative transmission without assigning physical locations to particles by stochastically modeling the free-path distribution between successive scattering interactions. In these simulations, the distances that photons travel before redirection are obtained via random draws from an analytic (usually exponential) free-path cumulative density function (CDF) based on the scatterer concentration of the medium. Modifications to propagation directions are obtained via random draws from an appropriate scattering phase-function (e.g. Henyey-Greenstein or Mie) describing the angular distribution of light intensity scattered by a particle for a given wavelength. This process of computing distance traveled prior to scattering, choosing a scattering angle, and re-computing distance traveled is repeated until all rays cast into the medium exit (based on specified "wall" boundary conditions).

In a ballistic 'photon' simulation [23,44], particles are placed in a volume at specified locations, and numerous rays are cast into the scattering medium [1,16]. Each ray is traced until it either exits the cloud on the other side unscattered (direct radiation) or its path intersects a particle (i.e., a geometric "collision"). The path of a scattered photon proceeds similar to those in the standard Monte Carlo algorithm outlined above; the new propagation direction is chosen from a phase function and subsequent scattering events can occur until the particle leaves the computational volume. Details associated with the computational implementation of this model are presented in the supplemental material.

This type of ballistic photon simulation allows particles to be placed anywhere in the volume to determine the impact of their spatial correlations on radiative transfer, but this benefit comes at the cost of recording and tracking a multitude of particle positions and collision locations. Though other approaches may resolve continuous media better [37], ballistic photon simulations are especially well-suited for spatially-correlated media where analytic extinction CDFs may not be known [44]. Our ballistic MCRT simulation extends the related numerical approach presented in Shaw et al. (2002) and Larsen and Clark [23] to a scattering domain. These simulations employ explicit positions for each individual particle within the medium, thus allowing for geometric ray-tracing to explore an arbitrary inter-scatterer distribution, rather than utilize a blind draw from a static (known) distribution function.

The simplest limiting case of this MCRT analysis occurs when simulating a cloud of monodisperse particles identically and independently distributed randomly within the simulation volume (see top panel of Fig. 2). Such a homogeneous system can serve as a control, where results can be validated against standard radiative transfer theory and expected analytic results. After validation on this simple (homogeneous) system, the MCRT code can be used to analyze virtual clouds comprised of non-uniform particle locations generated with the Matérn process described in the previous section (with an example of such a clustered distribution shown in the bottom panel of Fig. 2).

Rays (or 'photons') are initialized at uniformly-random (x, y, $z = 0$) positions and cast in a normally-incident collimated beam through one side of the volume, which contains numerous particles at specified (stationary) spatial locations. Intersections between these rays and particles create scattering events that modify the direction of each photon path; new ray directions are determined from the scattering phase function. Fig. S-3 in the supplemental material illustrates a subset of rays from a typical simulation result. In the case of cloud droplets with typical diameters larger than the wavelength of visible light, the resultant size parameter yields a scattering pattern that is forward-dominant.

The most rigorous way to calculate the scattering phase function is through Mie theory, where particles are considered as homogenous dielectric spheres interacting with an incident plane wave of light. However, it is convenient to have an analytic formula that approximates the actual scattering phase function shape, especially at this initial stage where details of the scattering are not expected to be as important for the scientific questions being explored. The Henyey-Greenstein phase function, essentially a probability density function (PDF) of scattering angle, is a common surrogate for the actual phase function [17]. Its analytic form allows it to be integrated to calculate a closed-form cumulative density function (CDF). Its parametric nature allows it to be employed rather simply, with sufficient accuracy for many applications [3,18,47]. The *mcScatter* software introduced here makes both Mie and HG (Henyey-Greenstein) phase functions available for scattering simulations.

As numerous rays are traced through the scattering medium, the locations of particle collisions and all individual ray segments are recorded. Direct and diffuse flux is recorded at a high spatial fidelity throughout the cloud depth, both backward and forward. This allows for direct, diffuse and total forward irradiance as well as backward irradiance to be calculated at many places within the cloud volume. Further details regarding the implementation of our scattering code beyond the basic phenomenological approach explained in this subsection can be found in the supplemental material.

3.2. Validation of MCRT direct beam extinction through a homogeneous uncorrelated medium

Before analyzing the impact of a spatially-correlated particle field on light scattering, we first ensured the fidelity of our MCRT code for non-scattering particles that are distributed with uniform probability (no spatial correlations). Given initial downward irradiance on a cloud top, F_0, the direct (unscattered) irradiance $F^{\downarrow}_{direct}$ is an exponential function of optical depth into the medium. By normalizing the direct, unscattered irradiance by the initial downwelling irradiance (where $\tau = 0$) we get an expression for the normalized direct flux [3] which can be written as

$$\varphi^{\downarrow}_{direct} = \frac{F^{\downarrow}_{direct}}{F_0} = exp(-\tau) \tag{3}$$

To calculate normalized direct flux with our MCRT code, we uniformly divide the expected total optical thickness into numerous "slabs". We represent total optical thickness as ($\tau^* = c\sigma z$), where c is the (number) concentration of scatterers, σ is the effective scattering cross section of each scatterer, and z is propagation depth through entire cloud. We then cast N_{ray} rays into the particle-laden medium and trace each ray to determine how may slabs are traversed before an absorbing particle is encountered. The number of rays passing each slab boundary is dependent on the total number of rays initially cast, but by dividing the tabulations by N_{ray} we compute a normalized optical depth-dependent direct flux. These direct beam extinction results were compared to the expected exponential decay to validate that portion of our MCRT code. One such comparison, performed for a monodisperse cloud with 14 µm radius particles and a total optical thickness (τ^*) of 1, is shown in Fig. 3. The simulation results matched the theoretical predictions exactly, with the expected exponential decay appearing linear due to the logarithmic y-axis.

3.3. Comparison of MCRT results to two-stream theory

One commonly made simplification is the idealization of radiative transfer into only two propagation directions, forward and backward [3,47]. This two-stream approximation is most accurate in the case of isotropic scattering where the phase function is uniform but can be used for anisotropic scattering as well with reasonable accuracy [47]. Thomas and Stamnes [47] state that, when Henyey-Greenstein phase function and two-stream approximations have been combined and compared to other (more accurate) methods, the resulting deviations are typically less than 2.5%, especially when the solar illumination is close to normally incident. For more information on the compromises made when using the Henyey-Greenstein phase function and multi-stream approximations the reader is referred to other works [27]. In order to place our MCRT results in a context that will be familiar to most readers, in this

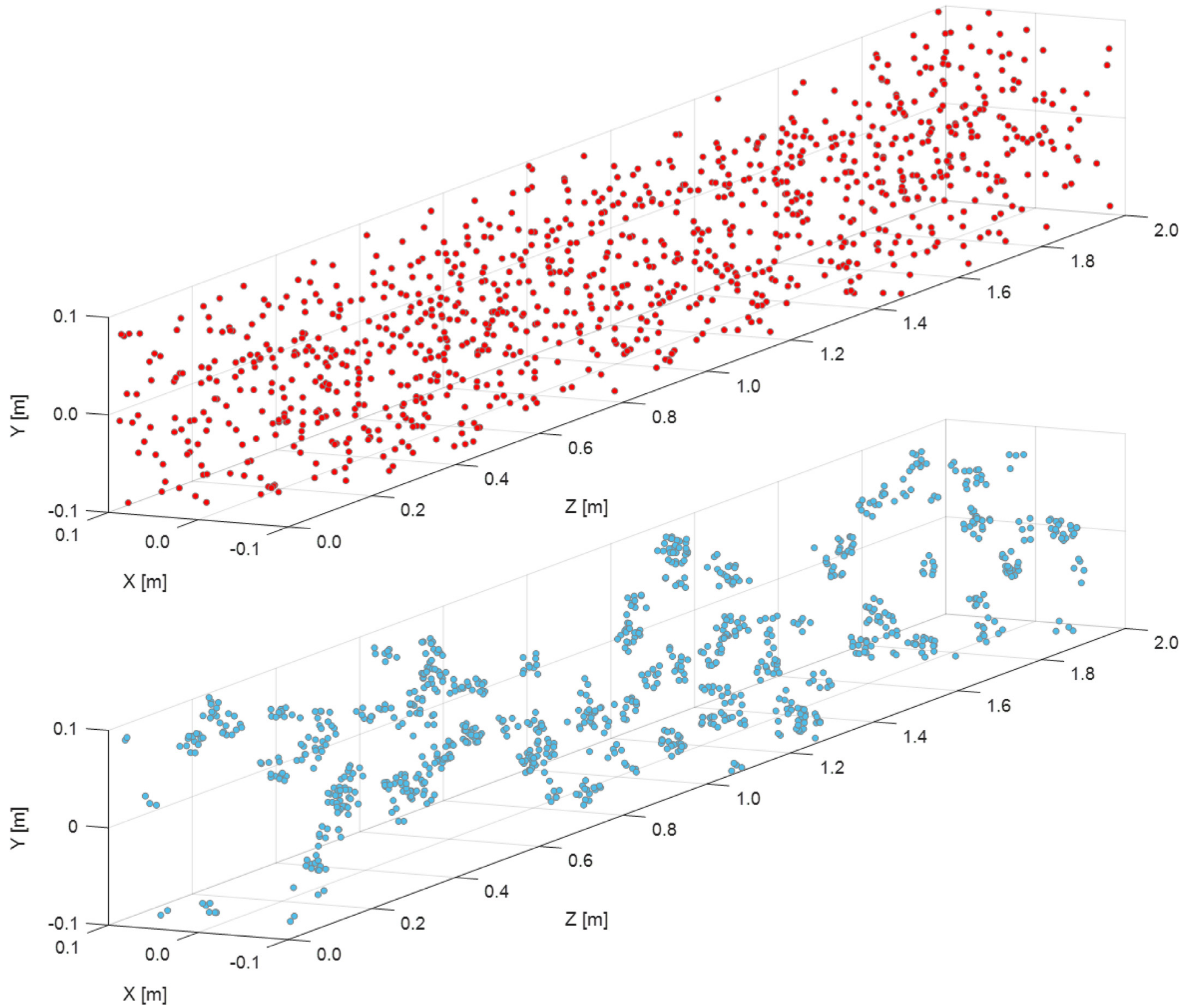

Fig. 2. Comparison between a homogeneous, uniform random particle distribution (top) and a Matérn-generated clustered distribution (bottom). Total cloud volume illustrated here and used for all scattering simulations in this works is 0.2 m x 0.2 m x 2.0 m (0.08 m^3).

subsection we compare them to the two-stream theory and then to Monte Carlo results presented in the textbook by Bohren and Clothiaux [3].

Using the Henyey-Greenstein phase function and periodic boundary conditions, each ray cast into the scattering medium continues moving either forward or backward until it terminates at the top or bottom of the simulated cloud. By normalizing the number of rays that cross each layer boundary (in either direction) by the total number of rays cast, the diffuse forward and backward flux components were computed. These MCRT simulation results were then compared to corresponding expressions from two-stream theory, such as the normalized diffuse forward flux given as [3]

$$\varphi^{\downarrow}_{diffuse} = \frac{D_{\downarrow}}{F_0} = \frac{1 + (\tau^* - \tau)\left(\frac{1-g}{2}\right)}{1 + \tau^*\left(\frac{1-g}{2}\right)} - \exp(-\tau) \tag{4}$$

and the normalized diffuse backward flux, expressed as

$$\varphi^{\uparrow}_{diffuse} = \frac{D_{\uparrow}}{F_0} = \frac{(\tau^* - \tau)\left(\frac{1-g}{2}\right)}{1 + \tau^*\left(\frac{1-g}{2}\right)} \tag{5}$$

In these normalized flux expressions, g refers to the asymmetry parameter, a scalar characterization of the degree of anisotropy calculated as the mean cosine of the scattering angle. Fig. 4 shows a comparison between two-stream theory curves for normalized forward and backward flux components and their Monte Carlo simulation counterparts. In this example, particles with a radius of 14 μm and a number density (n) of 400 cm^{-3} were used to create a homogeneous monodisperse random distribution with a total optical thickness (τ^*) of 1 with an asymmetry parameter (g) of 0.85.

The discrepancies evident in Fig. 4 between our MCRT results and two-stream theory are consistent with those suggested in Thomas and Stamnes [47] and shown in a similar comparison of two-stream theory with Monte Carlo by Bohren and Clothiaux [3].

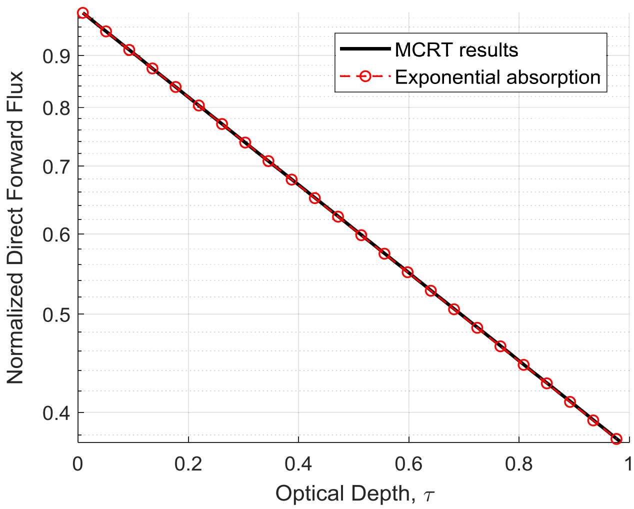

Fig. 3. Normalized direct, unscattered flux comparison between theoretical (circles) and Monte Carlo results (solid line) for a monodisperse cloud with 14 μm radius particles and τ^* of 1. Note that the vertical axis employs logarithmic spacing to illustrate exponential absorption.

These depth-dependent differences are due to the fact that two-stream theory approximates radiative transfer by neglecting the details that a full angular scattering solution includes. For validation purposes, the Monte Carlo results from Bohren and Clothiaux [3] are included in Fig. 4 for reference (circle and triangle symbols). We hypothesize that the slight differences between the Bohren and Clothiaux results and the MCRT results presented here are likely a result of details related to horizontal fluxes, such as the domain geometry and side-wall boundary conditions. As a further test, we used our MCRT code to simulate isotropic scattering ($g = 0.0$) and found excellent agreement with the transmission and reflectivity predictions of two-stream theory.

3.4. Simulation design for correlated random media

We emphasize here that the cluster sizes used in our analysis are smaller than the mean free path (as defined for a homogeneous medium), and therefore are not necessarily captured by a macroscopic, spatially varying mean free path. The radial distribution function depends on N_p and R, while the expected cloud optical thickness is $N_P \lambda_D V^{-1} Q_{sca} \pi a^2 L$ and thus depends on N_p, λ_D and particle radius a. It is therefore possible to explore the scattering problem under the constraint of fixed total optical thickness τ^* for varying input parameters, including those that directly influence the radial distribution function and therefore the magnitude and scale dependence of particle clustering.

Multiple particle cloud realizations were stochastically generated for each set of input parameters, and the results from each individual cloud scattering simulation were averaged together to form the reported (mean) optical depth-dependent fluxes. Due to the small cross sectional area being illuminated (0.2 m x 0.2 m), we found it necessary to analyze ten [10] unique clouds to compile trustworthy average flux results (see Fig. S-6 in the supplemental material). Consequently, all results shown in this work are the result of averaging the depth-dependent flux curves of at least ten unique cloud realizations, each of which was probed with 100,000 rays (see Fig. S-5 in the supplemental material).

4. Results

4.1. Impact of particle clustering on depth-dependent flux

In this work we investigate both the direct and diffuse radiative transfer (forward and backward) in a purely scattering but correlated random medium to determine expected deviations from commonly used radiative transfer predictions for a uniform, homogeneous medium. The problem depends on four parameters: N_p, R, λ_D and particle radius a. While the radial distribution function contains only N_p and R, the expected cloud optical thickness depends on N_p, λ_D and a. For our analysis we varied these four input parameters while constraining the total optical thickness τ^* to

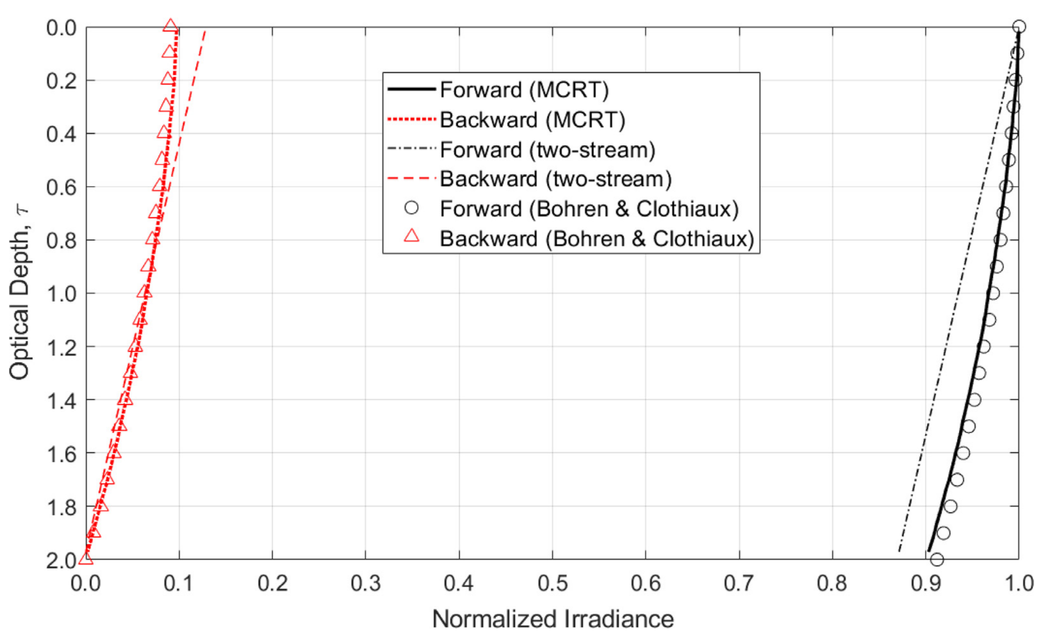

Fig. 4. Flux comparison between two-stream theory and Monte Carlo (MCRT) results, both forward flux (rightmost black curves) and backward flux (leftmost red curves). Note that at their most divergent, the two-stream and MCRT flux curves differ by 2–3%. Also shown for validation purposes are the Monte Carlo results (circle and triangle symbols) given in Bohren and Clothiaux [3], see top panel of their Fig. 6.10.

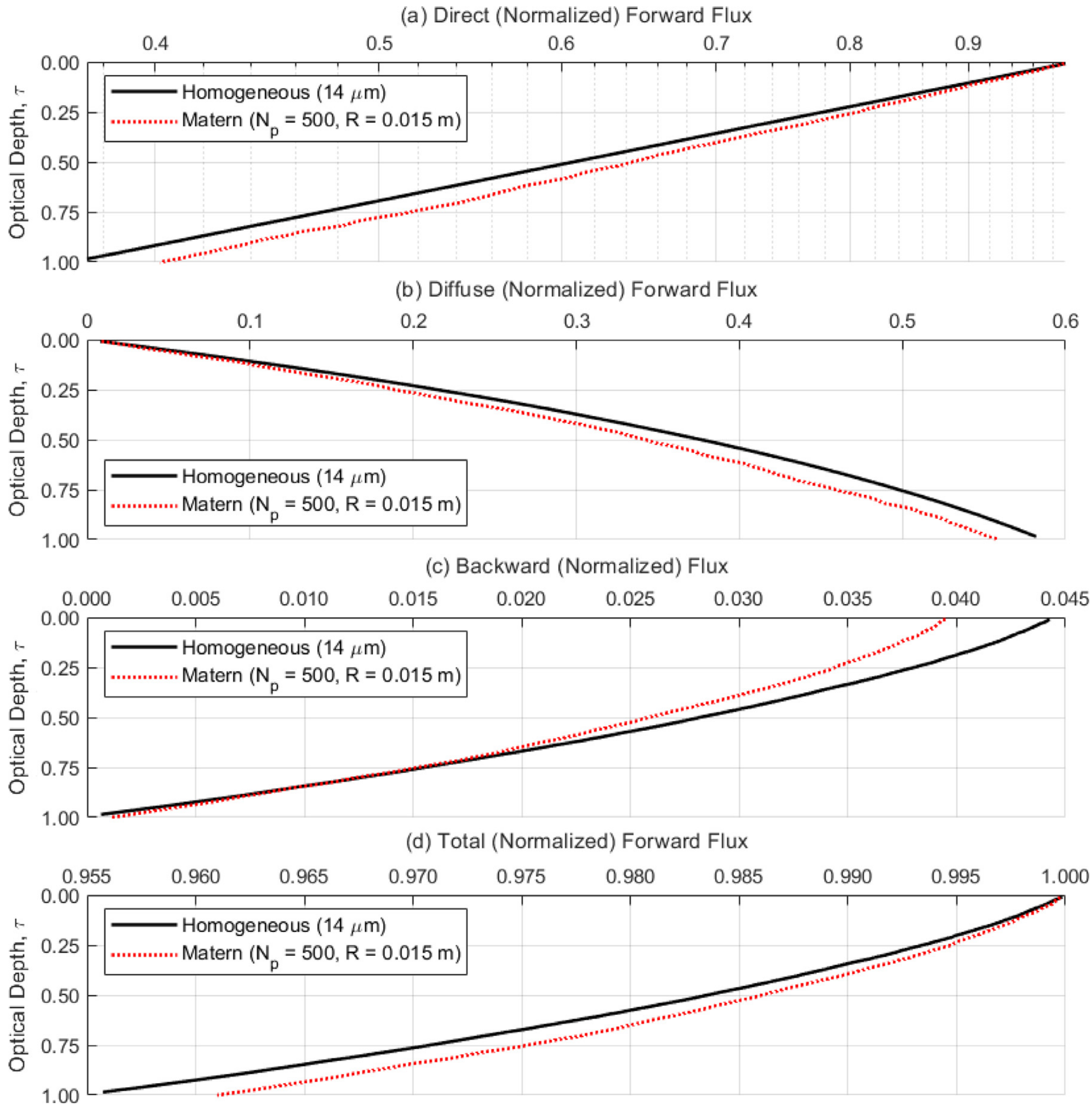

Fig. 5. Impact of particle clustering on depth-dependent flux curves as computed by our MCRT scattering simulation. Both homogeneous and Matérn correlated results were obtained from monodisperse (14 μm particle radius) cloud realizations with a total optical thickness, τ^*, of 1. Cluster radius, R, is 0.015 m and the number of cluster parents (N_p) is 500. The average number of particle per parent cluster (λ_D) is 64,000. Note that in this and subsequent figures, the independent variable optical depth (τ) increases downward on the reversed vertical axis, starting from the top of the cloud at $\tau = 0$ and finishing at the exit point at the bottom of the cloud ($\tau = 1$).

determine the influence of particle size, clustering and the radial distribution function.

We performed numerous scattering simulations through both uncorrelated and spatially-correlated monodisperse cloud distributions to explore the impact of spatial correlations on optical-depth-dependent irradiance. Mean optical depth-dependent irradiances, including direct and diffuse forward flux as well as backward flux, were calculated as a function of distance through both homogeneous and spatially correlated clouds. An example illustrating these various flux components is shown in Fig. 5, with the solid black line indicating the homogeneous case and the red dotted line indicating a Matérn-clustered scenario with ($N_p = 500$, $\lambda_D = 64{,}000$, $R = 0.015$ m). We note that the corresponding RDF is included as the dot-dashed red curve in Fig. 1.

When we consider the unscattered, direct flux traversing a simulated cloud, as shown in the top panel of Fig. 5 where τ increases downward on reversed vertical axis, we see that direct transmission is increased when spatial correlations exist in the particle-laden medium. Previous publications have shown that propagation through a spatially-correlated medium deviates from expectations of Beer-Lambert–Bouguer exponential attenuation [15,20,23,34,44]. Our Monte Carlo simulations, operating on clouds generated using a Matérn-process radial distribution function for particle positions, show this expected increase in direct flux through a field of particles. For the example in Fig. 5, at optical depth $\tau = 1$, an increase of direct transmission from 37% to more than 40% is observed in the Matérn-clustered results.

Note that while panel (a) of Fig. 5 shows an increase in direct transmission for the clustered compared to the unclustered distribution, panel (b) indicates a similar *decrease* in diffuse forward flux. Panel (c) indicates that, for this case, the amount of backward flux is slightly impacted by the existence of spatial correlation. Together these results signify that the difference in total forward flux (direct plus diffuse) due to spatial correlation, shown in panel (d) to be less than 0.5%, is only distinguishable when very tight normalized flux axis limits are chosen. In other words, when comparing only the mean normalized irradiances that would be detected at the bottom of the cloud, little difference would be measured, although presumably a radiance measurement separating direct from diffuse would reveal the distinction. Decreased direct attenuation is not totally compensated for by increased diffuse forward radiation, though they counterbalance to dampen the effect of particle clustering.

4.2. Impact of Matérn RDF parameters on depth-dependent flux

The Matérn RDF expression listed in Eq. (2) demonstrates dependency on both the number of parent clusters (N_p) and cluster radius (R). To test the hypothesis that these two parameters are the primary contributors to changes in depth-dependent flux for Matérn spatially correlated particle distributions, we simulated additional clustered clouds where these inputs were unchanged. The number of Matérn clusters was held constant at $N_p = 500$, and the cluster radius was fixed at $R = 0.0075$ m. While keeping N_p and R constant, we varied the monodisperse particle radius (e.g., 9.9 μm, 14 μm and 19.9 μm) and changed the mean number of particles per cluster accordingly (e.g., λ_D = 128,000, 64,000 and 32,000 respectively) to maintain a total optical depth of $\tau^* = 1$ for all simulated clouds. To ensure that we limited our exploration to parameters of interest, we enforced a constant asymmetry parameter and scattering efficiency (e.g., $g = 0.85$, and $Q_{sca} = 2.0$, respectively) in spite of changing particle radius.

As can be seen in Fig. 6, the three Matérn curves appear to collapse on each other. This supports the hypothesis that the N_p and R parameters, as with the underlying radial distribution function, are the driving factors impacting deviations from scattering theory for a homogeneous medium.

4.3. Variations in optical depth-dependent flux due to changes in Matérn clustering parameters

The optical depth-dependent irradiance results previously shown in Fig. 6 demonstrate a lack of dependence on changes to the clustering parameters absent from the Matérn RDF (namely, particle radius and mean number of particles per cluster, λ_D). We next investigate the impact of the parameters that are present in the Matérn RDF, namely cluster radius (R) and number of clusters (N_p). To determine the sensitivity of depth-dependent irradiance to cluster radius, we held all other quantities constant; 500 cluster parents with an average of 64,000 daughter particles of radius 14 μm were inserted using the Matérn process. Three cluster radii were explored ($R = 0.03$, 0.015 and 0.0075 m) and compared to the homogeneous (spatially-uncorrelated) case; the results are shown in Fig. 7. We see that as cluster radius decreases and the same number of particles are packed more densely, direct transmission is maximized and diffuse forward flux is minimized. Differentiation between the three Matérn curves is evident in both panel (a) and panel (b), illustrating the dependence on cluster radius R found in the RDF. We also note that there is a significant deviation of the backward diffuse flux for these Matérn cases as opposed to the homogeneous medium, as shown in panel (c); this ultimately results in a change in the total forward flux shown in panel (d).

Similarly, we explore the relationship between the number of cluster parents (N_p) and depth-dependent irradiance by constraining R and a, and allowing the average number of daughter particles per cluster, λ_D, to increase as N_p decreases to maintain constant expected optical thickness. The results of this investigation of constant cluster size R are shown in Fig. 8. We see that decreasing N_p increased the deviation from the spatially-uncorrelated case, supporting the notion that the optical-depth-dependent irradiance is impacted by a changing RDF. As can be seen from the dependence of the RDF expression on number of parents N_p and illustrated in Fig. 1, decreasing N_p with fixed R leads to an increase in the magnitude of the radial distribution function for all $r < 2R$. Once again, in Fig. 8 there is an observed departure of the backward flux from the homogeneous expectation.

The family of RDF curves shown in Fig. 1 were created by varying N_p and R, the two primary independent variables (beyond distance from cluster center, r); each of those nine RDF curves have a different $g(r = 0)$ peak correlation value. To explore the relevance of the shape of the Matérn RDF beyond just the peak correlation value, we study the impact of various RDF curves with equivalent $g(r = 0)$. Solving the Matérn RDF expression in Eq. (2) for the peak correlation value for $r = 0$ yields

$$g_{3D}(0) = \frac{3V}{4\pi R^3 N_p} + 1 \tag{6}$$

This means that for a given set of (R, N_p) input parameters, if R is doubled (or halved) and N_p is divided by (or multiplied by) eight, the peak correlation value $g(0)$ will be unchanged. We studied the impact of three Matérn RDFs with the same peak correlation value with this method, and the recorded depth-dependent flux curves are shown in Fig. 9. These results indicate that the impact of RDF on the radiative transfer depends on more than simply the peak correlation value, but also on the shape of the RDF itself. This confirms that both correlation strength and correlation length are relevant parameters.

5. Discussion and conclusions

5.1. Summary and interpretation of results

The presence of absorbing particles in a medium influences the direct radiative transfer through the medium, and the resulting optical transmissivity is dependent on the size and number of particles. However, if spatial correlations exist in particle locations, the resulting nonuniformities can lead to both clusters and voids on scales of the same order as or smaller than the optical mean free path (as defined for a uniform medium). In a purely absorbing medium, the net effect of these voids and clusters is to increase the direct radiative transfer through such a spatially-correlated medium, leading to sub-exponential extinction that deviates from the prediction of Beer-Lambert–Bouguer attenuation theory [20]. Conversely, negative spatial correlations (e.g., repelling particles) can lead to super-exponential extinction [44].

In the scattering-dominated limit, for which absorption is essentially non-existent, radiation is either transmitted directly (no interaction with particles in the medium) or diffusely (once a particle is encountered, the direction of propagation changes but the photon continues to traverse the medium). In this work, we have investigated direct and diffuse radiative transfer in a medium with spatially correlated scattering particles with a simplistic “ballistic photon” model. Our simulations explored the forward-dominant scattering regime that is typical of atmospheric clouds. The results are framed in the context of forward and backward fluxes, motivated by the commonly used two-stream flux equations.

Clustering was introduced using a Matérn clustering process with an analytical RDF to rigorously study the impact of four independent parameters, namely the number of clusters N_p, the cluster size R, the density of particles within a cluster λ_D, and the particle radius a. The parameter space was explored by constraining total optical depth τ^* to be 1 for all scattering simulations, and then considering various combinations of N_p, λ_D and a which together comprise the inputs to cloud optical thickness. Optical depth does not depend on cluster radius R, but the Matérn RDF depends on both R and N_p.

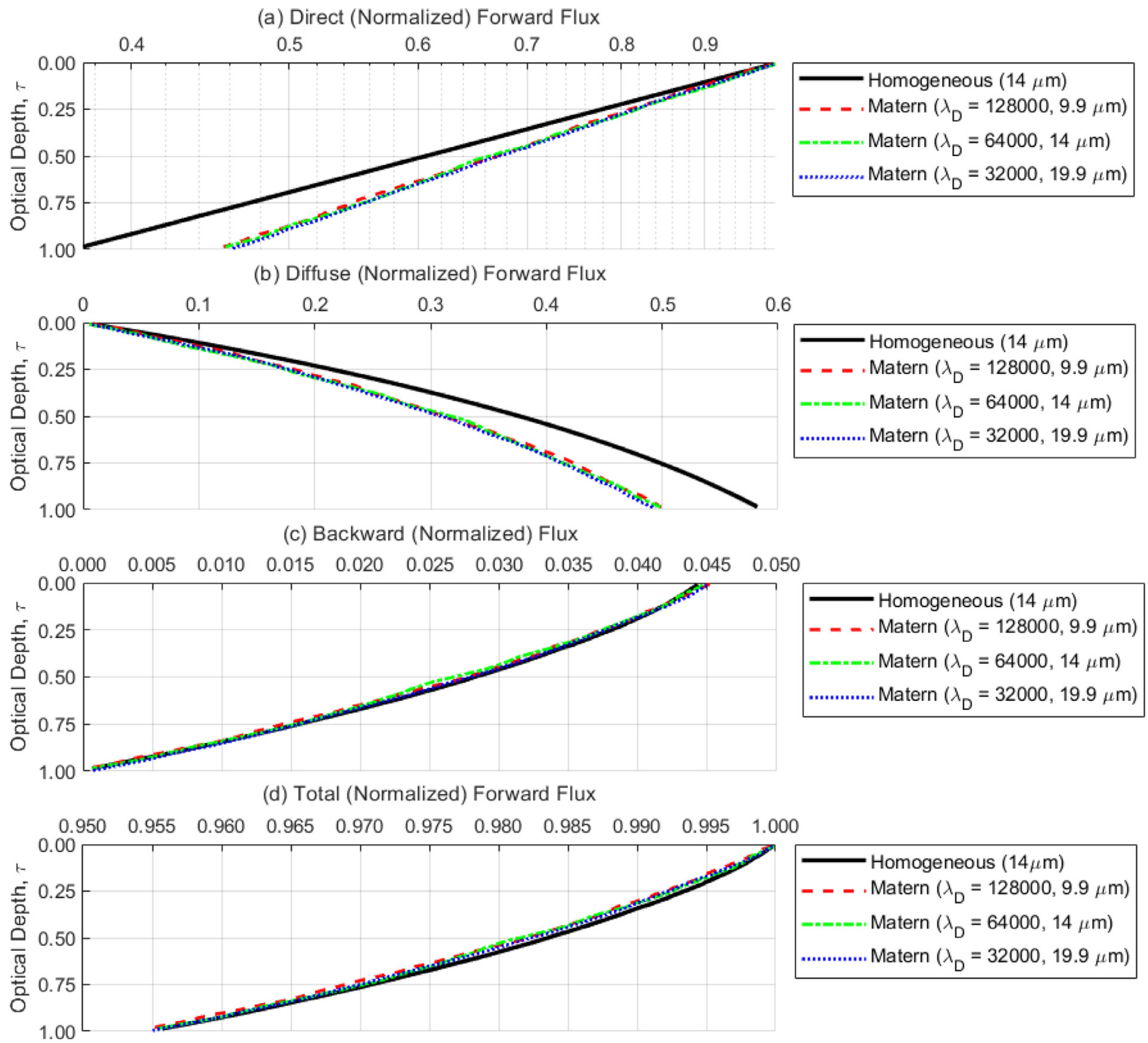

Fig. 6. Optical depth-dependent flux curves for a variety of Matérn-generated cloud distributions, with homogeneous particle distribution results shown for comparison. Note that in all three Matérn scenarios, the density of clusters and cluster radius are constant (e.g., $N_p = 500$ and $R = 0.0075$ m, respectively). Changes in monodisperse particle radius and number of mean particles per cluster (λ_D) have almost no impact on depth-dependent flux curves when N_p and R are held constant.

We found that particle clustering does indeed increase direct transmission, but we also found that diffuse forward irradiance is correspondingly reduced by a similar amount (Fig. 5). Additionally, we found that varying only parameters absent from the Matérn RDF (e.g., a and λ_D) had no statistical impact on depth-dependent flux recordings (Fig. 6). However, we determined that varying R and N_p (which are present in the RDF) did impact the irradiance results calculated by the scattering simulations (Figs. 7 and 8, respectively). Smaller clusters resulted in greater deviations from the direct and diffuse forward homogeneous baseline results, as did fewer but more densely packed parent clusters. Both of these conclusions are consistent with the hypothesis that these deviations are caused by voids in the scattering medium, and the heuristic prediction of the Beer-Lambert–Bouguer deviations developed by Kostinski [19,20]. For a constant total number of particles in a volume, both smaller clusters (all else equal) and fewer clusters result in larger voids and less (forward-dominant) scattering.

Lastly, we explored the relevance of the shape of the Matérn RDF beyond the peak correlation value (i.e., $r > 0$) by changing R and N_p in tandem to study the impact of various RDF curves with equivalent $g(r=0)$ peak values. We found that in addition to peak correlation value, the shape of the Matérn RDF is also significant, as evidenced by the varying depth-dependent flux curves in all four panels of Fig. 9. The Monte Carlo scattering simulations confirm that both correlation strength and correlation length are relevant parameters for predicting radiative transfer in a spatially correlated particle-laden medium.

Some insight can be gained from considering the relevant length scales in this radiative transfer problem. There are at least four scales: particle radius a, cluster size R that can be referred to as the correlation length scale, the photon mean free path defined for the volume-average properties $l \approx 1/(nQ_{sca}\pi a^2)$, and the box size L. In this work L has been fixed and constrained to be equal to l, such that $\tau^\star = 1$ for all cases. The clustering or correlation length R in all cases explored here is smaller than l. The results show that both the correlation length and the strength of correlation, expressed for example through $g(r=0)$ (cf., Eq. (6) for the relationship with N_p), determine the extent to which optical propagation and scattering deviate from the theoretical prediction for domain-average properties.

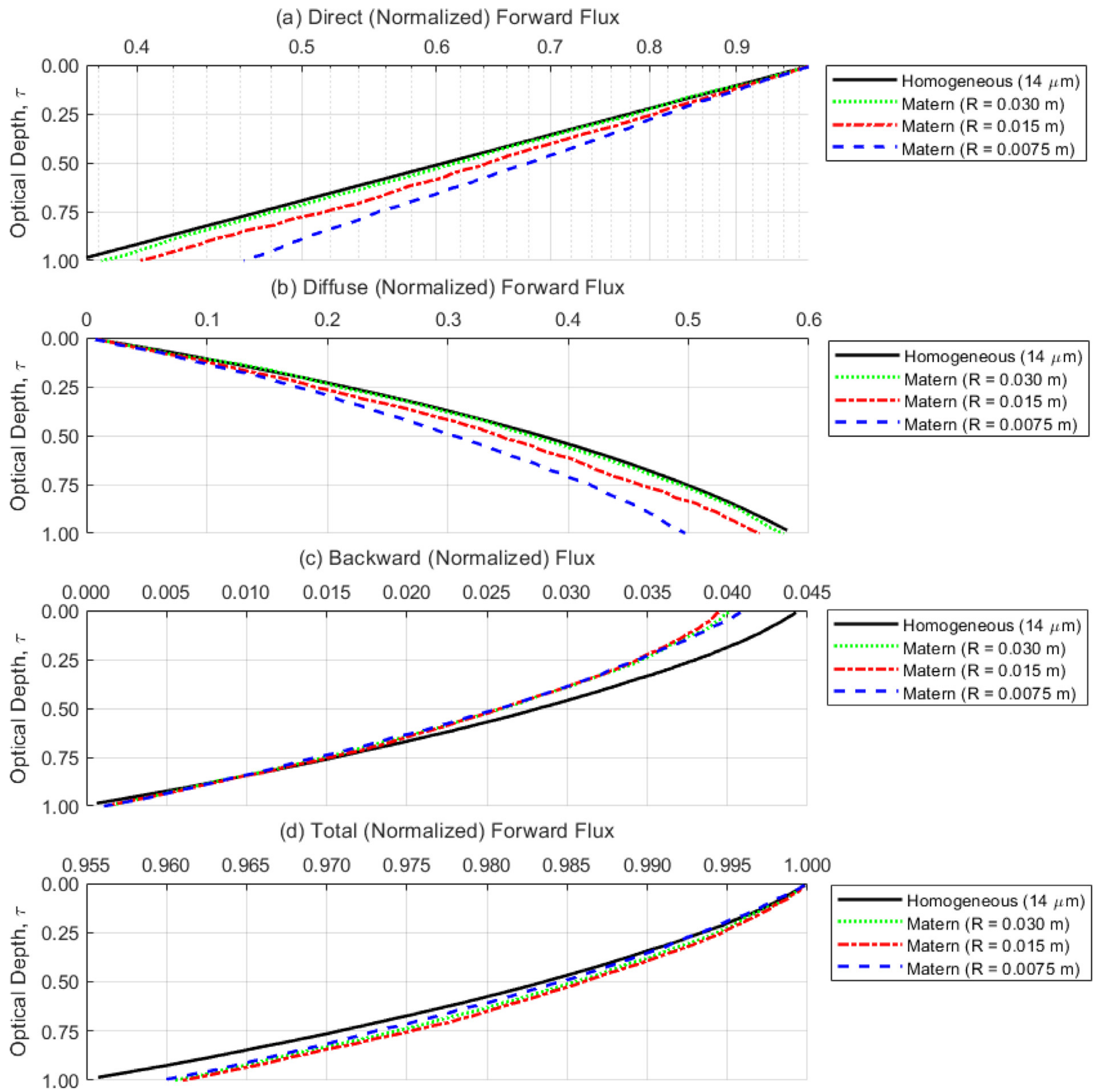

Fig. 7. Optical depth-dependent flux curves for a variety of Matérn-generated cloud distributions, with homogeneous particle distribution results shown for comparison. All virtual cloud distributions are monodisperse with 14 μm particle radius. Note that in all three Matérn scenarios, the density of clusters and mean number of particles per cluster are constant (e.g., $N_p = 500$ and $\lambda_D = 64{,}000$, respectively).

5.2. Results in context with prior work

Previous work [23,39] has gone into detail on trying to understand the inter-relationships between length scales in this problem. For purely absorptive media, Larsen and Clark [23] used numerical simulations to reveal that at least three different length-scales will be relevant – particle size, correlation length-scale, and optical mean-free-path between particles. The work of Petty [39] also has similarities to the approach presented here, with the "cloudlets" designed in that model similar in structure to the individual Matérn clusters in our simulation. Petty's approach employs a non-dimensional parameter τ' (referred to as the effective mean optical thickness of a cloudlet) to attempt to capture all relevant information about small scale variability necessary to resolve the deviations from expected Beer-Lambert–Bouguer exponential transmission. For our Matérn-clustered clouds, this τ' parameter can be expressed as

$$\tau' = \frac{3Q_{sca}a^2\lambda_D}{2R^2} \tag{7}$$

In Petty's notation the effective optical thickness, which accounts for enhancement in transmission due to non-uniform distribution of liquid water, is expressed as $\tau^*_{eff} = \varphi(\tau')\sigma\bar{W}$ where $\phi(\tau')$ is the optical depth reduction factor and $\bar{W}$ is the average liquid water path. This can be written as $\tau^*_{eff} = \varphi(\tau')\bar{n}Q_{sca}\pi a^2 L$ where $\bar{n}$ is the domain-averaged number density. In terms of Matérn parameters, the mean volumetric number density is $\bar{n} = N_p\lambda_D V^{-1}$, allowing us to write the effective optical thickness as $\tau^*_{eff} = \varphi(\tau')N_p\lambda_D V^{-1}Q_{sca}\pi a^2 L$. Petty's cloudlet optical thickness can be expressed as $\tau' = 3Q_{sca}a^2\lambda_D(2R^2)^{-1}$, but since we constrained the global optical thickness through constant $\bar{n}$ we can rewrite that as $\tau' = 3Q_{sca}a^2\bar{n}V(2R^2N_p)^{-1}$. This is an intriguing result because we can now see that we have the same variable depen-

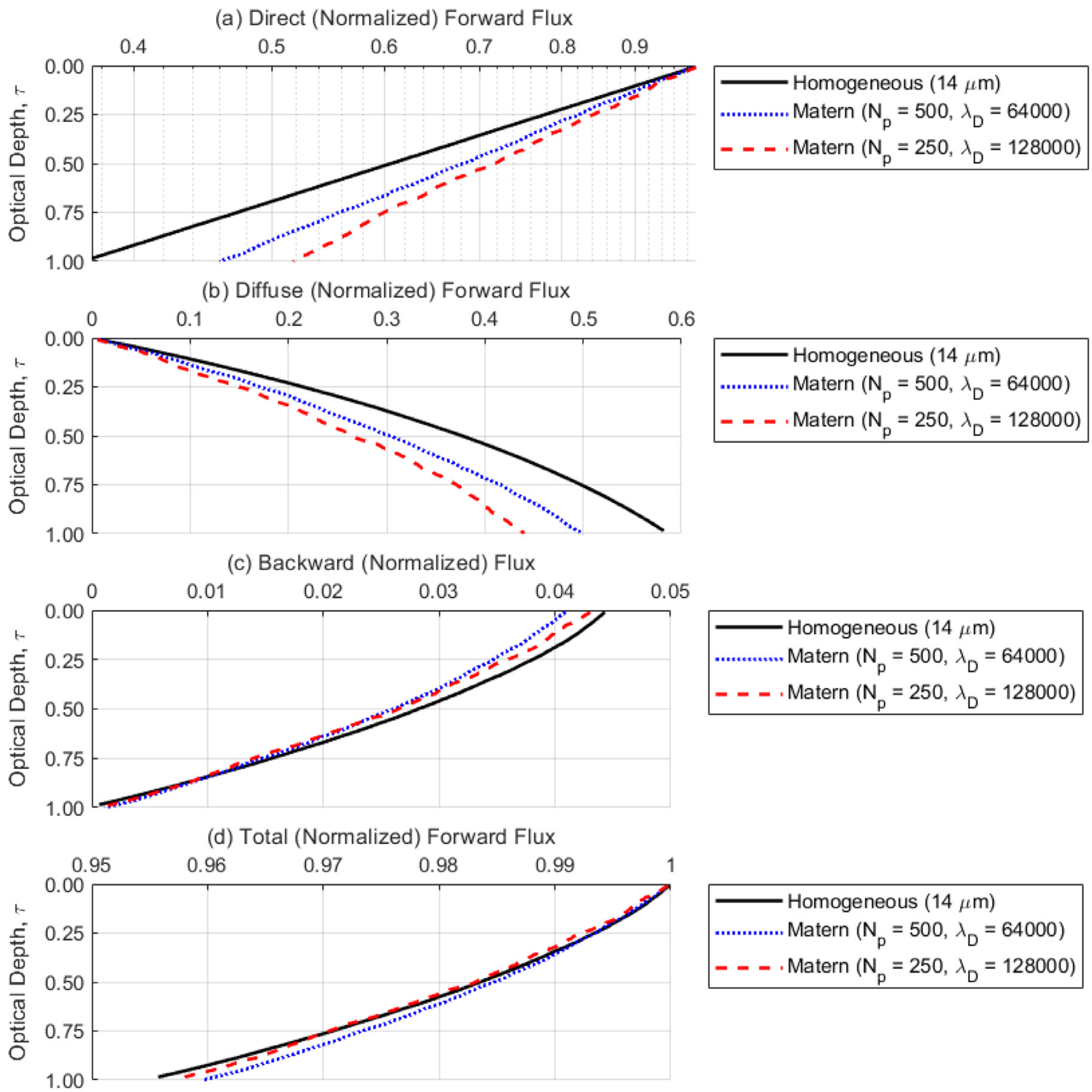

Fig. 8. Optical depth-dependent flux curves for a variety of Matérn-generated cloud distributions, with homogeneous particle distribution results shown for comparison. All virtual cloud distributions are monodisperse with 14 μm particle radius. Note that for both Matérn scenarios, cluster radius is constant (e.g., $R = 0.0075$ m).

dence, i.e. N_p and R, as seen in our Matern RDF in Eq. (2). Given this encouraging similarity, we computed $\phi(\tau')$ and τ^*_{eff} for the conditions in all of our simulations to compare predictions of direct, non-exponential transmission. The results of this comparison (see Fig. 10) show reasonable agreement between our Monte Carlo results and the cloudlet model, suggesting that the Matérn RDF is consistent with the cloudlet approach. Because of the connection between the RDF and traditional, continuous correlation functions [45], this RDF-based work can serve as a bridge between the two approaches: radiative transfer calculations based on continuous correlation functions [4,15] and those based on the analytical results from the clearly-visualized cloudlet model. The RDF has the advantage that it has a direct link to discrete particle distributions, and it is general in the sense that it can describe more than Matérn or cloudlet models. For example, analytical expressions exist for less defined forms of clustering, beyond the Matérn notion of spherical particle clouds surrounded by voids (e.g., modified Thomas, Gibbs systems, excluded volume, etc.). The links identified here open the door for exploring to what extent other RDF expressions are able to facilitate comparison of Monte Carlo results, and furthermore suggest that it should be possible to find a quantitative link between $\phi(\tau')$ and the RDF.

A renormalization technique for predicting radiative transfer for inhomogeneous clouds was proposed by Cairns et al. whereby single scattering parameters are modified based on spatial variances in scatterer concentration for use with plane-parallel calculations [5]. They propose that for random, purely scattering media where the correlation length is of the same order as the mean free path, an augmented extinction cross section and asymmetry parameter can be computed as

$$\begin{aligned} \sigma'_{ext} &= \sigma_{ext}(1+V_{rel})^{-1} \\ g' &= g[1+V_{rel}(1-g)]^{-1} \end{aligned} \tag{8}$$

where V_{rel} is the relative variance of scatterer concentration. When spatially-varying scatterer concentration $N(r)$ is comprised of a mean concentration $\bar{N}$ and zero-mean fluctuating component $\eta(r)$, as in

$$N(r) = \bar{N} + \eta(r), \tag{9}$$

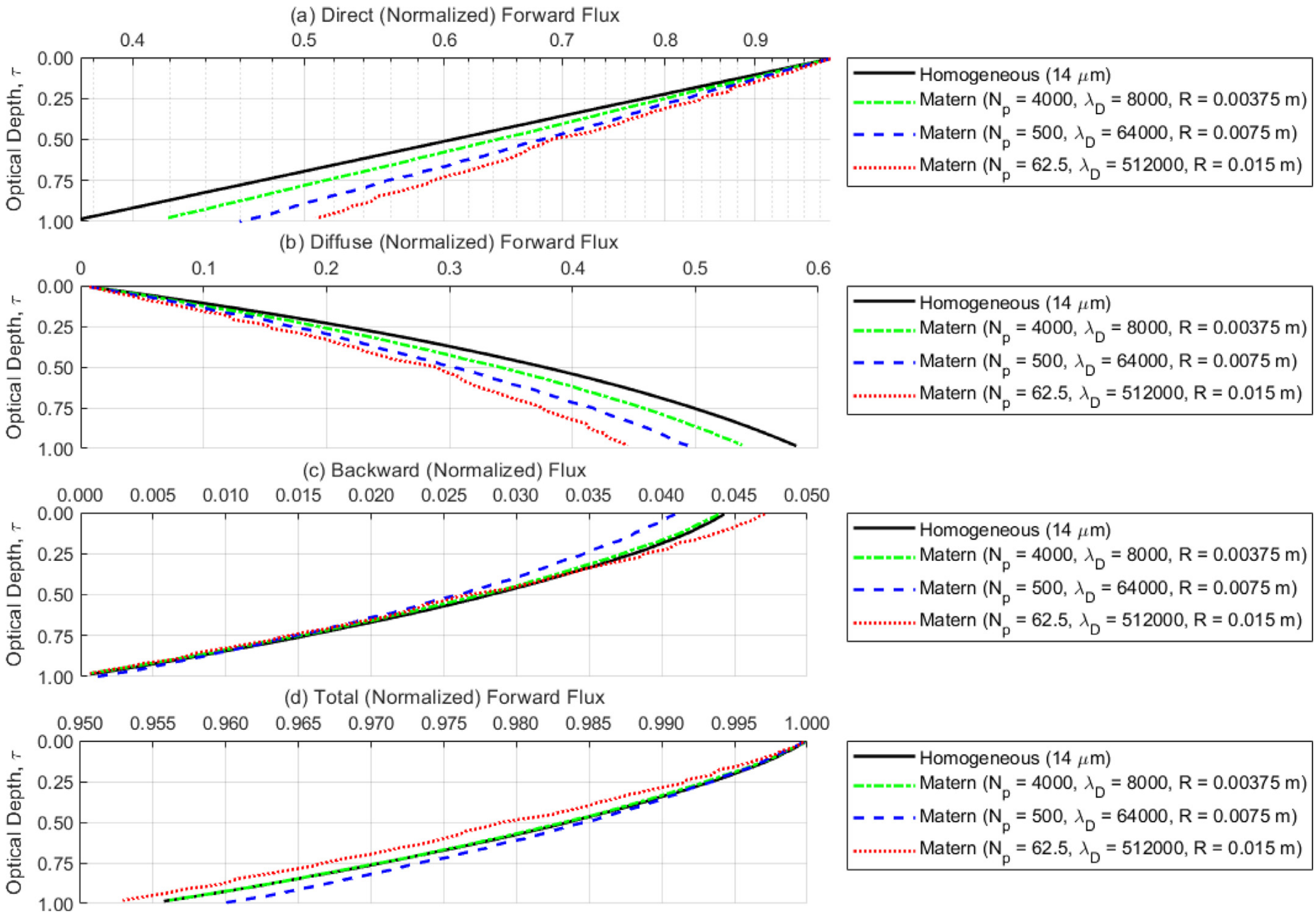

Fig. 9. Matérn scattering results from three combinations of N_p and R, both present in the RDF and varied together to achieve a constant RDF at $g(r = 0)$, are compared. Note that λ_D was changed in correspondence with N_p to ensure a constant τ^* of 1.

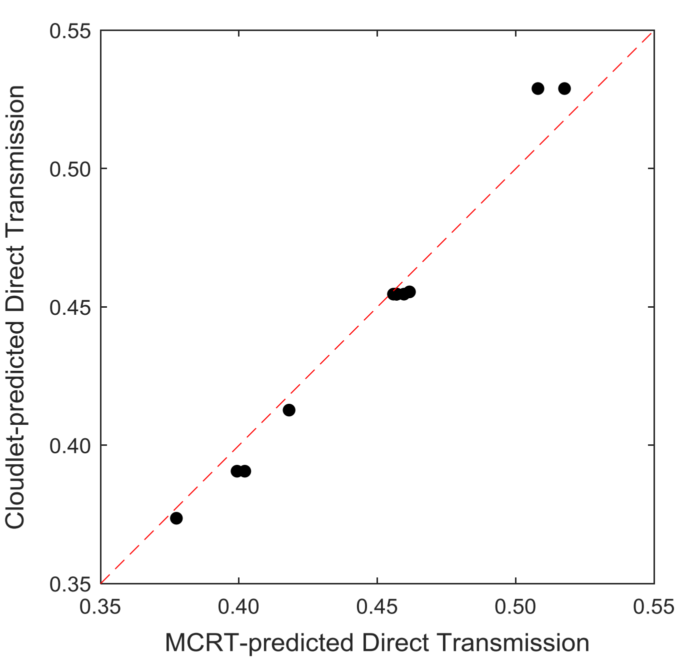

Fig. 10. Comparison of direct, non-exponential transmission through spatially correlated particle distribution.

relative variance can be expressed as

$$V_{rel} = \eta(r)^2\ \bar{N}^{-2} \tag{10}$$

For our analysis, the average scatterer concentration is simply the total number of scatterers divided by the simulation volume. The variance calculations will depend on how the simulation volume is subdivided, i.e., it will be scale dependent. The number of scatterers in each subvolume can be used to compute $\eta(r)$ and ultimately V_{rel}. For example, when 32 × 10^6 particles are grouped into 500 parent clusters with an average of 64,000 particles per cluster (of radius 7.5 mm), dividing the 0.08 m^3 volume into ten subvolumes along the path of the direct beam yields a small relative variance of 1×10^{-2}; division into 1000 cubic subvolumes (e.g., 10 × 10 × 10) results in a larger relative variance of 1.3. These values of V_{rel} lead to modified asymmetry parameter g' values of 0.849 and 0.711 (respectively) and modified scattering efficiency Q'_{sca} values of 1.98 and 0.87 (respectively). In the former case, where the scattering parameters are only slightly augmented, the MCRT results match those of the homogeneous case (where $g = 0.85$ and $Q_{sca} = 2.0$) and do not predict the direct and diffuse forward flux deviations seen in the Matérn clustering simulation. In the latter case, where the scattering parameters are heavily modified by the calculated relative variance, total optical thickness is greatly reduced (from 1.0 to 0.425, due to a reduced Q_{sca}) and none of the various flux components are predictive of the Matérn-based MCRT results. This serves to illustrate the dependence of averaging scale when considering a system of discrete particles. Here we have considered correlation lengths smaller than the mean free path, and it should be noted again that this is outside the range explored by Cairns et al. [5].

5.3. Concluding remarks and implications

It is reasonable to consider the implications of this work for radiative transfer in the cloudy atmosphere, as a specific example of a particulate system that possesses spatial correlations over a large range of scales. The influence of spatial inhomogeneity on three-dimensional radiative transfer has been considered in depth, for the limit in which the scale of the inhomogeneity is larger than the mean free path defined for the medium. The pioneering work of Kostinski [20] makes clear, however, that fundamental assumptions of the continuum approach to radiative transfer are called into question when correlations in a discrete-particulate medium are considered. Indeed, in atmospheric clouds typical mean free paths for regimes dominated by scattering (e.g., visible light) are of order 100 m, so essentially the entire turbulence inertial subrange lies at smaller scales. Therefore, entrainment and mixing processes generate strong spatial correlations in droplet positions from the ∼100-m energy injection scale to the ∼1-mm dissipation scale, and inertial clustering generates spatial correlations from the ∼1-cm scale down to the ∼10 µm scale of a single particle diameter [49,50]. The question of how these sub-free-path-scale correlations might influence radiative transfer has been studied by several groups for the absorbing-particle limit [15,20,23,44]. In this work we have explored the regime in which light scattering is dominant, and specifically for particles larger than the illuminating wavelength for which forward scattering is pronounced; this is the relevant regime for atmospheric clouds and visible/near-IR radiation. The results of the study suggest that the degree to which there is a deviation from standard radiative transfer using the medium-averaged optical properties (e.g., mean free path) can be quantified through the radial distribution function. This implies that knowledge of the RDF resulting from inertial clustering and turbulent mixing in atmospheric clouds would be valuable [26]. Treatment of the RDF is a first step, as a two-particle correlation function, and eventually it will be insightful to consider the possible relevance of multi-particle correlations on light propagation.

This work has focused on the influence of clustering at scales below the mean free path of the radiation, for optical depths up to order unity. Implications for larger scales such as would be relevant to cloud remote sensing or energy budgets will require consideration of cloud organization at the full range of scales: for example, it is already widely appreciated that clustering on spatial scales large compared to the photon mean free path is of significance in practical applications. It is known, however, that the turbulent energy cascade stretches down to the 1 mm scale in the atmosphere, so clouds can be assumed to be non-uniform far below the scale of a mean free path. The next stage of this work is validation of the MCRT results directly with measurements in the Pi cloud chamber. Characterization of actual clustering strength in natural clouds will be required to put the chamber measurements into atmospheric context. This kind of comparison will allow the overall approach of MCRT methods to be assessed; although they are widely used in applied radiative transfer, they are known to neglect the detailed electromagnetic treatment that is potentially necessary for full representation of propagation in a correlated medium (e.g., [37]). Experimental results will be the ultimate arbiter.

In some cases presented here, the changes to direct and diffuse radiation are nearly compensating; do such results suggest that there is no significance to the clustering? That depends on the problem under consideration: for any problem depending on directional properties of the radiation field, the details of direct versus diffuse will be of significance. It is a subject that will be investigated in subsequent, combined computational and experimental work. Indeed, the geometry chosen in this study was originally motivated by the desire to explore the extent to which optical propagation through a turbulent cloud can be studied in the laboratory. That has the advantage of allowing well-characterized cloud and turbulence conditions, as well as statistically homogeneous and stationary conditions needed for spatial and temporal averaging. The sensitivity actually required in a study of this phenomenon, for realistic turbulence and clustering levels, will be the subject of future work, but the results presented here suggest that measurement of the cloud particle RDF will be a necessary step in possible experiments.

Acknowledgments

We thank Benjamin Bandt-Horn, Eric Marttila and James Truax of ThermoAnalytics, Inc. for their insightful suggestions regarding the practical implementation of current computer graphics methodologies for efficient ray tracing. We are grateful to Craig Bohren, Eugene Clothiaux, and Peter Pilewskie for helpful conversations about Monte Carlo versus 2-stream results. This material is based on research sponsored by Air Force Research Laboratory (AFRL) under agreement number FA9453-16-1-0083, as well as National Science Foundation (NSF) grants AGS-1532977 and AGS-1823334. The U.S. Government is authorized to reproduce and distribute reprints for Governmental purposes notwithstanding any copyright notation thereon. The views and conclusions contained herein are those of the authors and should not be interpreted as necessarily representing the official policies or endorsements, either expressed or implied, of Air Force Research Laboratory (AFRL) or the U.S. Government.

Supplementary materials

Supplementary material associated with this article can be found, in the online version, at doi:10.1016/j.jqsrt.2019.106601.

References

[1] Banko AJ, Villafañe L, Kim JH, Esmaily M, Eaton JK. Stochastic modeling of direct radiation transmission in particle-laden turbulent flow. J Quant Spectrosc Radiat Transf 2019;226:1–18. https://doi.org/10.1016/j.jqsrt.2019.01.005.

[2] Barker HW. Solar radiative transfer through clouds possessing isotropic variable extinction coefficient. Q J R Meteorol Soc 1992;118:1145–62. https://doi.org/10.1002/qj.49711850807.

[3] Bohren CF, Clothiaux EE. Fundamentals of atmospheric radiation: an introduction with 400 problems. Weinheim: Wiley-VCH; 2011.

[4] Borovoi AG. Radiative transfer in inhomogeneous media. Dokl Akad Nauk SSSR 1984;276:1374–8.

[5] Cairns B, Lacis AA, Carlson BE. Absorption within inhomogeneous clouds and its parameterization in general circulation models. J Atmos Sci 2000;57:700–14. https://doi.org/10.1175/1520-0469(2000)057⟨0700:AWICAI⟩2.0.CO;2.

[6] Chang K, Bench J, Brege M, Cantrell W, Chandrakar K, Ciochetto D, Mazzoleni C, Mazzoleni LR, Niedermeier D, Shaw RA. A laboratory facility to study gas-aerosol-cloud interactions in a turbulent environment: the Π chamber. Bull Am Meteorol Soc 2016 https://doi.org/10.1175/BAMS-D-15-00203.1.

[7] Chiu SN, Stoyan D, Kendall WS, Mecke J. Stochastic geometry and its applications. 3rd ed. Chichester: Wiley; 2013.

[8] Chun J, Koch DL, Rani SL, Ahluwalia A, Collins LR. Clustering of aerosol particles in isotropic turbulence. J Fluid Mech 2005;536:219–51. https://doi.org/10.1017/S0022112005004568.

[9] Cole JNS. Assessing the importance of unresolved cloud-radiation interactions in atmospheric global climate models using the multiscale modelling framework Doctoral Thesis. Department of meteorology, The Pennsylvania State University; 2005.

[10] Collins DG, Blättner WG, Wells MB, Horak HG. Backward monte carlo calculations of the polarization characteristics of the radiation emerging from spherical-shell atmospheres. Appl Opt 1972;11:2684–96. https://doi.org/10.1364/AO.11.002684.

[11] Danielson RE, Moore DR, van de Hulst HC. The transfer of visible radiation through clouds. J Atmos Sci 1969;26:1078–87. https://doi.org/10.1175/1520-0469(1969)026⟨1078:TTOVRT⟩2.0.CO;2.

[12] Davis AB. Effective propagation kernels in structured media with broad spatial correlations, illustration with large-scale transport of solar photons through cloudy atmospheres. In: Graziani F, editor. Computational methods in transport, lecture notes in computational science and engineering. Berlin Heidelberg: Springer; 2006. p. 85–140.
[13] Davis AB, Marshak A. Photon propagation in heterogeneous optical media with spatial correlations: enhanced mean-free-paths and wider-than-exponential free-path distributions. J Quant Spectrosc Radiat Transf 2004;84:3–34. https://doi.org/10.1016/S0022-4073(03)00114-6.
[14] Davis AB, Marshak A, Gerber H, Wiscombe WJ. Horizontal structure of marine boundary layer clouds from centimeter to kilometer scales. J Geophys Res Atmos 1999;104:6123–44. https://doi.org/10.1029/1998JD200078.
[15] Frankel A, Iaccarino G, Mani A. Optical depth in particle-laden turbulent flows. J Quant Spectrosc Radiat Transf 2017;201:10–16. https://doi.org/10.1016/j.jqsrt.2017.06.029.
[16] Frankel A, Iaccarino G, Mani A. Convergence of the Bouguer–Beer law for radiation extinction in particulate media. J Quant Spectrosc Radiat Transf 2016;182:45–54. https://doi.org/10.1016/j.jqsrt.2016.05.009.
[17] Henyey LG, Greenstein JL. Diffuse radiation in the galaxy. Astrophys J 1941;93:70–83. https://doi.org/10.1086/144246.
[18] Ishimaru A. Wave propagation and scattering in random media. New York; Oxford; New York: IEEE Press ; Oxford University Press; 1997.
[19] Kostinski AB. On the extinction of radiation by a homogeneous but spatially correlated random medium: reply to comment. JOSA A 2002;19:2521–5. https://doi.org/10.1364/JOSAA.19.002521.
[20] Kostinski AB. On the extinction of radiation by a homogeneous but spatially correlated random medium. JOSA A 2001;18:1929–33. https://doi.org/10.1364/JOSAA.18.001929.
[21] Landau LD, Lifshitz EM. Statistical physics. Oxford, UK: Butterworth-Heinemann; 1980.
[22] Larsen EW, Vasques R. A generalized linear boltzmann equation for non-classical particle transport. J Quant Spectrosc Radiat Transf 2011;112:619–31. 2009 International Conference on Mathematics and Computational Methods (M&C 2009) https://doi.org/10.1016/j.jqsrt.2010.07.003 .
[23] Larsen M, Clark A. On the link between particle size and deviations from the Beer-Lambert–Bouguer law for direct transmission. J Quant Spectrosc Radiat Transf 2014;133:646–51. https://doi.org/10.1016/j.jqsrt.2013.10.001.
[24] Larsen ML, Briner CA, Boehner P. On the recovery of 3D spatial statistics of particles from 1D Measurements: implications for airborne instruments. J Atmos Ocean Technol 2014;31:2078–87 https://doi.org/10.1175/JTECH-D-14-00004.1.
[25] Larsen ML, Shaw RA. A method for computing the three-dimensional radial distribution function of cloud particles from holographic images. Atmos Meas Technol 2018;11:4261–72. https://doi.org/10.5194/amt-11-4261-2018.
[26] Larsen ML, Shaw RA, Kostinski AB, Glienke S. Fine-Scale droplet clustering in atmospheric Clouds: 3D radial distribution function from airborne digital holography. Phys Rev Lett 2018;121:204501. https://doi.org/10.1103/PhysRevLett.121.204501.
[27] Li J, Barker H, Yang P, Yi B. On the aerosol and cloud phase function expansion moments for radiative transfer simulations. J Geophys Res Atmos 2015;12:142. 120128-12 https://doi.org/10.1002/2015JD023632 .
[28] Lu J, Nordsiek H, Saw EW, Shaw RA. Clustering of charged inertial particles in turbulence. Phys Rev Lett 2010;104:184505. https://doi.org/10.1103/PhysRevLett.104.184505.
[29] Marchuk GI, Mikhailov GA, Nazaraliev MA, Darbinjan RA, Kargin BA, Elepov BS. The Monte Carlo methods in atmospheric optics. Springer; 1980 https://doi.org/10.1007/978-3-540-35237-2.
[30] Marshak A, Davis AB. 3D radiative transfer in cloudy atmospheres. Berlin: Springer; 2005.
[31] Martínez VJ, Saar E. Statistics of the galaxy distribution. CRC Press; 2002.
[32] Matérn B. Spatial variation. Lecture notes in statistics. 2nd ed. New York: Springer-Verlag; 1986.
[33] Matérn B. Poisson processes in the plane and related models for clumping and heterogeneity, NATO Advanced Study Institute on Statistical Ecology. Pennsylvania State University; 1972.
[34] Matsuda K, Onishi R, Kurose R, Komori S. Turbulence effect on cloud radiation. Phys Rev Lett 2012;108:224502. https://doi.org/10.1103/PhysRevLett.108.224502.
[35] Mishchenko MI. Multiple scattering, radiative transfer, and weak localization in discrete random media: unified microphysical approach. Rev Geophys 2008:46. https://doi.org/10.1029/2007RG000230.
[36] Mishchenko MI. Radiative transfer in clouds with small-scale inhomogeneities: microphysical approach. Geophys Res Lett 2006:33. https://doi.org/10.1029/2006GL026312.
[37] Mishchenko MI, Dlugach JM, Yurkin MA, Bi L, Cairns B, Liu L, Panetta RL, Travis LD, Yang P, Zakharova NT. First-principles modeling of electromagnetic scattering by discrete and discretely heterogeneous random media. Phys. Rep. 2016;632:1–75. First-principles modeling of electromagnetic scattering by discrete and discretely heterogeneous random media https://doi.org/10.1016/j.physrep.2016.04.002 .
[38] Packard CD, Shaw RA, Cantrell WH, Kinney GM, Roggemann MC, Valenzuela JR. Measuring the detector-observed impact of optical blurring due to aerosols in a laboratory cloud chamber. J Appl Remote Sens 2018;12:042404. https://doi.org/10.1117/1.JRS.12.042404.
[39] Petty GW. Area-Average solar radiative transfer in three-dimensionally inhomogeneous clouds: the independently scattering cloudlet model. J Atmos Sci 2002;59:2910–29. https://doi.org/10.1175/1520-0469(2002)059⟨2910:AASRTI⟩2.0.CO;2.
[40] Plass GN, Kattawar GW. Monte carlo calculations of light scattering from clouds. Appl Opt 1968;7:415–19. https://doi.org/10.1364/AO.7.000415.
[41] Reade WC, Collins LR. Effect of preferential concentration on turbulent collision rates. Phys Fluids 2000;12:2530–40. https://doi.org/10.1063/1.1288515.
[42] Saw E-W, Shaw RA, Salazar JPLC, Collins LR. Spatial clustering of polydisperse inertial particles in turbulence: II. Comparing simulation with experiment. New J Phys 2012;14:105031. https://doi.org/10.1088/1367-2630/14/10/105031.
[43] Shaw RA. Particle-turbulence interactions in atmospheric clouds. Annu Rev Fluid Mech 2003;35:183–227. https://doi.org/10.1146/annurev.fluid.35.101101.161125.
[44] Shaw RA, Kostinski AB, Lanterman DD. Super-exponential extinction of radiation in a negatively correlated random medium. J Quant Spectrosc Radiat Transf 2002;75:13–20. https://doi.org/10.1016/S0022-4073(01)00287-4.
[45] Shaw RA, Kostinski AB, Larsen ML. Towards quantifying droplet clustering in clouds. Q J R Meteorol Soc 2002;128:1043–57. https://doi.org/10.1256/003590002320373193.
[46] Sobol' IM, Chicago Univ Il. Department of mathematics. The Monte Carlo method. Popular lectures in mathematics. The University of Chicago Press; 1974.
[47] Thomas GE, Stamnes K. Radiative transfer in the atmosphere and ocean. Cambridge; New York: Cambridge University Press; 1996.
[48] Warhaft Z. Passive scalars in turbulent flows. Annu Rev Fluid Mech 2000;32:203–40. https://doi.org/10.1146/annurev.fluid.32.1.203.
[49] Wyngaard JC. Turbulence in the atmosphere. Cambridge, UK; New York: Cambridge University Press; 2010.
[50] Wyngaard JC. Atmospheric turbulence. Annu Rev Fluid Mech 1992;24:205–34. https://doi.org/10.1146/annurev.fl.24.010192.001225.
[51] Zoller CJ, Hohmann A, Foschum F, Geiger S, Geiger M, Ertl TP, Kienle A. Parallelized monte carlo software to efficiently simulate the light propagation in arbitrarily shaped objects and aligned scattering media. J Biomed Opt 2018;23:1–12. https://doi.org/10.1117/1.JBO.23.6.065004.